Ultrasonic Assisted Electrochemical Trepanning of Rectangular Groove with Inner Cylindrical Structure

Chun-Hao Yang [1], Tzu-Yuan Chu [1], A-Cheng Wang [2], Yan-Cherng Lin [3], and Hai-Ping Tsui [1,*]

[1] Department of Mechanical Engineering, National Central University, Taiwan
[2] Department of Mechanical Engineering, Chien Hsin University of Science and Technology, Taiwan
[3] Department of Vehicle Engineering, Nan Kai University of Technology, Taiwan
Email: bon.jason@gmail.com (C.-H.Y.); sd2323zz@gmail.com (T.-Y.C.); acwang@uch.edu.tw (A.-C.W.); ycline@nkut.edu.tw (Y.-C.L.); benno@ncu.edu.tw (H.-P.T.)
*Corresponding author

***Abstract*—In the process of Electrochemical Machining (ECM), the electrolyte renewal is likely to be poor as the machining gap is too narrow, so that the machining accuracy and surface quality are influenced, especially in the electrochemical trepanning of special structures, such as the rectangular groove with inner cylinder. As the flow field in the machining gap is difficult to be uniform, the machining quality is low and the cylindrical taper angle is large. Based on the abovementioned difficulties in ECM process, this study used ECM with mask and ECM with tool sinking, as well as the methods with and without ultrasonic vibration assisted sidewall-insulated electrodes, to conduct a comparative experiment on the electrochemical trepanning of rectangular groove with inner cylindrical structure for SUS304 stainless steel cylindrical workpieces. This study also discussed the effects of different ECM trepanning processing methods on the quality characteristics, such as cylindrical taper angle and surface morphology. The research results showed that in comparison to the ECM with mask, ECM with tool sinking had a smaller cylindrical taper angle and better surface morphology. When the ultrasonic vibration assistance was used for ECM with tool sinking, the uniformity of the flow field was improved. The electrolyte pressure changed rapidly in the processing area with the ultrasonic vibration assistance, resulting in pumping effect and cavitation effect, both of which disturbed the electrolyte, and promoted the renewal of the electrolyte in the machining gap. As a result, the resistance within the machining area is reduced, a smaller cylindrical taper angle was obtained, and the flow marks at the bottom of the rectangular groove were significantly reduced. Moreover, the surface morphology and surface roughness of the rectangular groove with inner cylinder after processing were better.**

***Keywords*—electrochemical trepanning, rectangular groove with inner cylinder, ultrasonic vibration assistance, sidewall-insulated electrode**

I. Introduction

As the demand for processing advanced materials grows gradually, the Electrochemical Machining (ECM) technology has attracted widespread attention from the industrial circles for its advantages. At present, the ECM technology has been widely used in aerospace, semiconductor, automobile and biomedical industries. It has become the preferred technology for processing super alloys and the parts of difficult-to-machine materials [1, 2]. However, the ECM technology also has its challenges. One of them is that the sidewall of the processed structure is likely to form an excessive taper angle. As the front end of the workpiece is processed earlier than the rear end of the workpiece in the feeding process of ECM, and the electrolyte renewal is poor, the upper end of the workpiece is often subject to more anodic corrosion than the bottom. In order to solve the above-mentioned processing difficulties, some studies used a gas film or suction head to confine the electrolyte within a range to prevent it from splashing and causing stray corrosion [3, 4], while other studies adopted various methods to insulate the tool electrode sidewall, so as reduce the stray corrosion induced by the electrode sidewall [5–7]. Other studies used nanosecond-scale ultra-short pulse voltage [8, 9], special feed modes [10], and low-frequency electrode vibration [11, 12] or rotating spiral electrodes [13] to overcome the problem of poor electrolyte renewal.

A number of studies applied ultrasonic to ECM surface finishing, drilling and micro-milling to solve the problem of poor electrolyte renewal, so as to improve the surface roughness [14–16]. Others used ultrasonic vibration semi-cylindrical tool electrodes [17], composite ultrasonic vibration electrodes [18], and ultrasonic vibration-assisted microarray electrodes [19] for ECM drilling, which could greatly improve the processing speed and accuracy. According to experiments and numerical simulations, scholars found that the ultrasonic vibration changed the conditions of electrochemical dissolution, and reduced the polarization of the electrode under the optimal vibration amplitude [20].

Manuscript received February 15, 2024; revised May 5, 2024; accepted May 21, 2024; published November 8, 2024.

In addition, for the ECM trepanning structure, some studies applied ultrasonic to the flowing electrolyte and used pulse current for ECM processing. The surface roughness of the workpiece was reduced, and the taper angle of the processed workpiece was reduced significantly [21]. As for the ECM trepanning structure without ultrasonic assistance, previous studies optimized and improved the electrode morphology through flow field simulation analysis [7, 22], or explored different electrolyte supply methods, hoping to improve the stability of the machining process and the accuracy of the products [23].

This study aims to solve the problem that the sidewall of the cylindrical structure is likely to form an excessive taper angle after the electrochemical trepanning of rectangular groove with inner cylindrical structure. In the experiment, the epoxy resin was used as an insulating material to cover and insulate the inner hole sidewall of the tool electrode to produce a sidewall-insulated electrode. The electric field was concentrated at the front end of the tool electrode to increase the machining current density and reduce the stray corrosion phenomena in ECM. The tool electrode was used for ECM with mask and ECM with tool sinking comparative experiment. The comparative experiment was conducted on the electrochemical trepanning of rectangular groove with inner cylindrical structure for SUS304 stainless steel cylindrical workpieces. In addition, a comparative experiment on the machining with and without ultrasonic vibration assisted sidewall-insulated electrode was performed. When the ultrasonic-assisted vibrating tool electrode was used for electrochemical trepanning of rectangular groove with inner cylindrical structure, the ultrasonic vibrating tool electrode could bring pumping effect and cavitation effect. The former one forms a squeezing effect in the machining gap, while the latter one produces micro-jets. These mechanisms can accelerate the cyclic renewal of the electrolyte in the machining gap, so as to effectively remove such machining bi-products as metal oxides, bubbles, and reaction heat generated during machining, as well as to improve the machining accuracy and avoid excessive taper angle of the cylindrical structure. This study used the better results after comparing the ECM with mask with the ECM with tool sinking, and then conducted the comparative experiment on the electrochemical trepanning of rectangular groove with inner cylindrical structure with and without ultrasonic vibration assisted method. The effects of different processing methods on the quality characteristics such as cylindrical taper angle and surface morphology also be discussed.

II. Principles of Experiments

A. Principle of Ultrasonic

The sidewall-insulated electrode is vibrated by an ultrasonic tool holder in this experiment. The vibrated sidewall-insulated electrode promotes a pumping effect and a cavitation effect in the electrolyte. The aforementioned two effects are explained as follows.

1) Pumping effect

As the electrolyte is incompressible, when the tool electrode vibrates up and down in the machining gap, the electrolyte is disturbed and compressed, so that the electrolyte is extruded from and sucked into the machining gap, generating the pumping effect, as shown in Fig. 1.

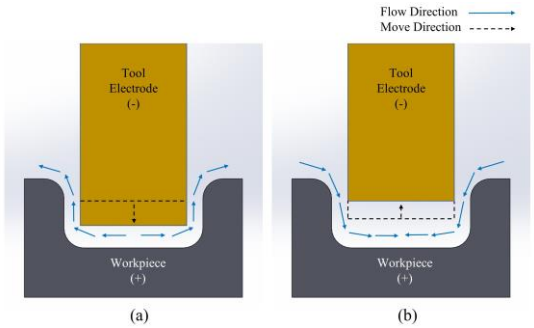

Fig. 1. Schematic diagram of ultrasonic pumping effect. (a) Tool electrode moving downward; (b) Tool electrode moving upward.

2) Cavitation effect

When ultrasonic waves propagate in fluids, they cause rapid changes in the medium pressure. When the pressure is lower than the saturated vapor pressure, the liquid begins to boil and generate bubbles. These bubbles are called cavitation bubbles, and their internal pressure is close to vacuum. As the medium pressure rises, the cavitation bubbles suddenly collapse, so that the peripheral liquid rushes into the center, producing a small but powerful micro-jets.

III. Experimental Settings

A well-scripted methods sections lays the foundation for your research by outlining the different methods you used to derive your results. The methods used to achieve the objectives must be described precisely and in sufficient detail, so as to allow a competent reader to repeat the work done by the author.

A. Experimental Materials

1) Stainless steel cylindrical workpiece

The workpiece used in this experiment was a cylindrical SUS 304 stainless steel material with a diameter of 16 mm and a height of 13 mm, as shown in Fig. 2. The chemical composition of the workpiece is shown in Table I.

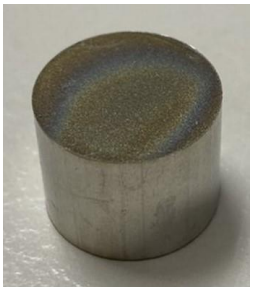

Fig. 2. Photo of cylindrical SUS 304 stainless steel.

TABLE I. CHEMICAL COMPOSITION OF THE WORKPIECE

Chemical composition	Proportion (wt. %)
Carbon, C	0.08
Chromium, Cr	18.0–20.0
Iron, Fe	68.0–70.0
Manganese, Mn	2.0
Nickel, Ni	8.0–10.5
Nitrogen, N	0.1
Silicon, Si	1.0
Others	≦0.1

2) Sidewall-insulated electrode

The sidewall-insulated electrode used in this experiment is shown in Fig. 3, and the photo of epoxy resin insulated part of the sidewall-insulated electrode is shown in Fig. 4. In addition to the front copper sheet of this electrode that can conduct electricity for ECM trepanning, the insulated part in the figure and the inner wall of the hole were insulated with epoxy resin. The quick connector locked in the middle of the electrode was used to connect the electrolyte supply hose, so that the electrolyte was supplied from the center of the electrode, and the screw locked at the rear was used to lock the power cord, so as to connect the negative electrode of the power supply. The specification of the sidewall-insulated electrode is shown in Table II and the chemical composition of the electrode is shown in Table III.

3) Electrolyte

This experiment used sodium nitrate ($NaNO_3$) as the electrolyte. Compared with other electrolytes, the aqueous solution of $NaNO_3$ was neutral, so its corrosiveness to the equipment was relatively low. In addition, the nitrate ions in the solution formed a passivation layer on the workpiece, which can improve the processing accuracy.

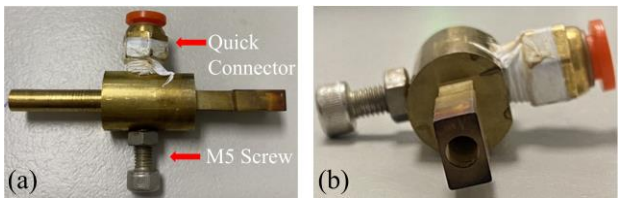

Fig. 3. Photo of sidewall-insulated electrode. (a) Side view; (b) Front view.

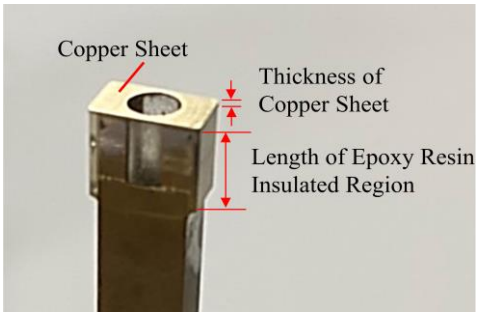

Fig. 4. Photo of epoxy resin insulated part of the sidewall-insulated electrode.

TABLE II. THE SPECIFICATION OF THE SIDEWALL-INSULATED ELECTRODE

Specification	Description
Full length (mm)	73.3
Copper sheet size (mm × mm)	9×5.4
Hole diameter of copper sheet (mm)	4.3
Thickness of copper sheet (mm)	0.3
Length of epoxy resin insulated region (mm)	17
Quick connector	PT-1/8″
Screw size	M5

TABLE III. CHEMICAL COMPOSITION OF THE ELECTRODE

Chemical composition	Proportion (wt. %)
Copper, Cu	62.0–65.0
Zinc, Zn	34.0–38.0
Others	≦0.5

B. Experimental Instruments

Schematic diagram of the experimental setup is shown in Fig. 5. The Z-axis with a servo motor can move up and down, and the ultrasonic tool holder is settled on the Z-axis and can produce high-speed vibration in the Z-direction. The sidewall-insulated electrode was locked on the ultrasonic tool holder, and the workpiece was settled in the electrolytic tank. The electrolyte was filtered through the electrolyte circulation system, the temperature was controlled, and then it was pumped by the pressure pump into the sidewall-insulated electrode, so that the electrolyte can be supplied downward from the center of the tool electrode. The processing power supply was a DC power supply with a signal generator and IGBT transistor to generate pulse power, and was connected to the tool electrode (cathode) and workpiece (anode) for constant current power supply. When the two electrodes are connected to a power source and energized in the electrolyte, electrochemical reactions occur at the electrodes. The electrochemical reaction equations at the two electrodes are as follows:

Anode:

$$\mathrm{Fe} \rightarrow \mathrm{Fe}^{2+} + 2e^- \quad (1)$$

$$\mathrm{Fe}^{2+} + 2OH^- \rightarrow \mathrm{Fe(OH)_2} \downarrow \quad (2)$$

$$4Fe(OH)_2 + 2H_2O + O_2 \rightarrow 4Fe(OH)_3 \downarrow \quad (3)$$

Cathode:

$$2H^+ + 2e^- \rightarrow \mathrm{H}^2 \uparrow \quad (4)$$

The electrode (cathode) does not participate in the reaction; only hydrogen gas is generated on its surface.

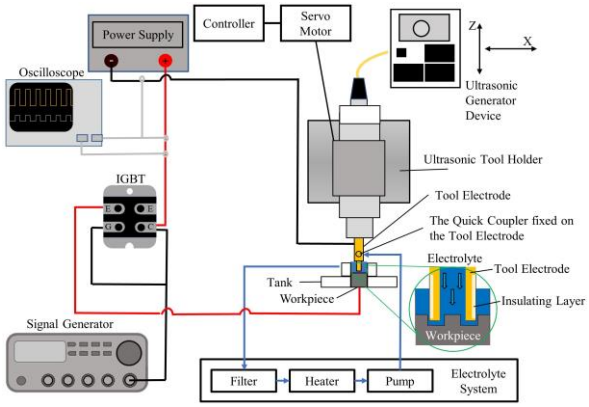

Fig. 5. Schematic diagram of the experimental setup.

C. Measurement and Observation on Experimental Results

The physical appearance of the rectangular groove with inner cylinder processed in this experiment is shown in Fig. 6. The processing quality characteristics, including the cylindrical taper angle and surface roughness, were measured using a laser confocal and white light interferometry. The center point of the cylinder was determined in the built-in height multi-point circle building mode, and then the built-in section line function of the measurement software was used. If the section line passes through the center point of the cylinder and was parallel to the long side of the rectangular groove, the section view of the cylinder could be obtained, and then the cylindrical taper angle could be measured.

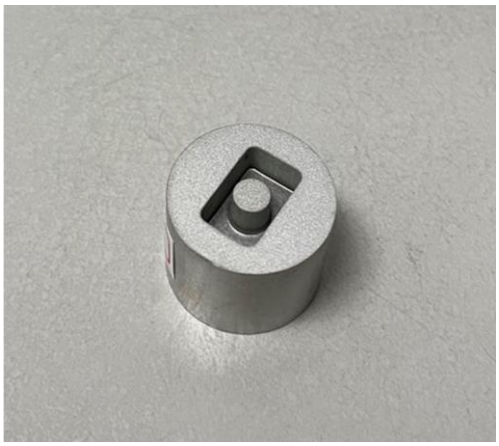

Fig. 6. Physical appearance of the rectangular groove with inner cylinder.

1) Cylindrical taper angle measurement

In the ECM, the taper angle (t_i) is an important indicator to evaluate the machining quality. Considering the fillet of the top surface and root of the cylinder, the taper angle was measured 3 mm down from 0.4 mm away from the top surface, as shown in Fig. 7. The computing equation of the taper angle t_i is expressed as follows:

$$t_i = \arctan\left(d_B/3\right) \quad (5)$$

where d_B is the width deviation within the measurement distance.

As the taper angle can be measured on two sides of one section, the cylindrical taper angle is the average of the measured values on both sides. The equation is expressed as follows:

$$t = \frac{1}{2}\sum_{i=1}^{2} t_i \quad (6)$$

where t_i is the taper angle on one side of the cylindrical section measured by the laser confocal and white light interferometer, where t is the cylindrical taper angle.

Fig. 7. Photo of cylindrical taper angle measurement.

2) Observation on surface morphology of rectangular groove with inner cylindrical structure

The stereomicroscope in this study was used to observe and photograph the overall 3D morphology of the processed rectangular groove with inner cylinder.

IV. Result and Discussion

A. Influence of ECM with Mask and ECM with Tool Sinking on Electrochemical Trepanning of Rectangular Groove with Inner Cylinder

First, this study used a DC power supply to conduct ECM with mask and ECM with tool sinking experiments, and discussed the effect of different ECM methods on the quality characteristics, such as the cylindrical taper angle and the surface morphology of the rectangular groove with inner cylinder. The ECM with mask covered a mask on the workpiece, under the mask shielding effect, the electrochemical reaction area occurred in the unshielded area of the mask. The ECM with tool sinking used a tank that can accommodate the electrolyte. The area of electrochemical reaction between the workpiece and the sidewall-insulated electrode was all in the tank, and this area was covered with the electrolyte. Fig. 8 shows the experimental setup photos of the said two ECM methods. Fig. 8 (a) is the initial position of tool electrode of the ECM with mask (b) is the tool electrode lifting position of the ECM with mask (c) is the initial position of tool electrode of ECM with tool sinking (d) is the tool electrode lifting position of the ECM with tool sinking. This section discusses the effect of using the two ECM methods on the quality characteristics of electrochemical trepanning of rectangular groove with inner cylinder. The processing parameter settings are shown in Table IV.

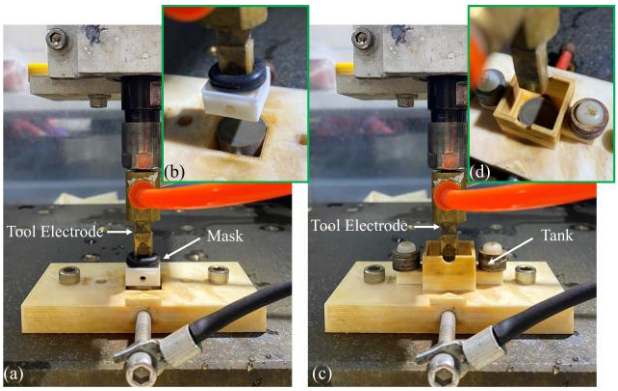

Fig. 8. The experimental setup photos of two ECM methods. (a) Initial position of tool electrode of the ECM with mask. (b) Tool electrode lifting position of the ECM with mask. (c) Initial position of tool electrode of ECM with tool sinking. (d) Tool electrode lifting position of the ECM with tool sinking.

TABLE IV. THE PARAMETERS AND SETTING VALUES OF THE EXPERIMENTS

Parameters	Description
Machining current (A)	18, 18.5, 19
Electrode feed rate (μm/s)	7.5
Initial working gap (μm)	60
Electrode feeding stroke (μm)	3940
Current mode	Direct current
Tool electrode polarity	(–)
Electorlyte concentration (wt.%)	10
Electrolyte temperature (°C)	30
Electrolyte supply pressure (psi)	2.5
Ultrasonic vibration frequency (kHz)	0

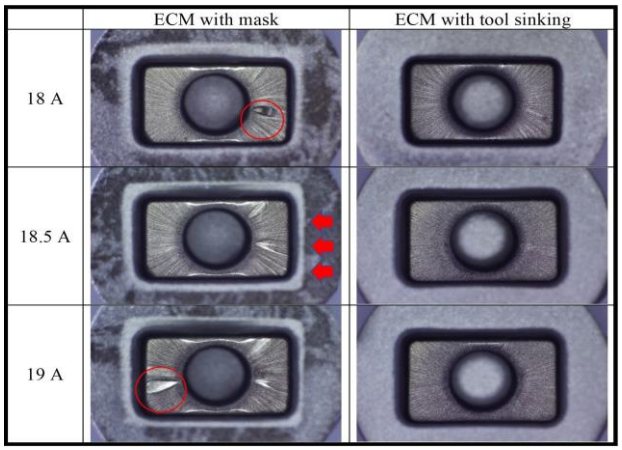

Fig. 9. The surface morphology of the rectangular groove with inner cylinder processed by different ECM methods.

Fig. 9 shows the surface morphology of the rectangular groove with inner cylinder processed by different ECM methods under different machining current. As seen, the bottom morphology of the rectangular groove processed by ECM with mask is poor and large pits are prone to appear, as indicated by red circles. In addition, the top edge of the workpiece processed by ECM with mask is relatively white. Because the surface of the workpiece inside the mask is covered with the electrolyte and is affected by stray corrosion. The surface of the workpiece covered by the mask does not contact the electrolyte, so it is not affected by stray corrosion, and shows the original color of the workpiece. Finally, a color difference is formed on the surface of the workpiece, as indicated by the red arrow. As shown in Fig. 9, the rectangular groove with inner cylinder processed by immersion processing has better surface morphology.

Fig. 10 shows the relationships between different processing methods and the cylindrical taper angle. As seen, in the two processing methods, as the machining current increases from 18 A to 19 A, the cylindrical taper angle of the ECM with mask increases from 1.934° to 2.301°, while the cylindrical taper angle of ECM with tool sinking increases from 1.891° to 2.139°. The cylindrical taper angles of the two processing methods increase with the machining current. Because the increase in current causes the increase in ECM capability, and the top material is electrochemically processed for a long time, so that the amount of material removed from the top of the cylinder is greater than that from the bottom of the cylinder, and the cylindrical taper angle increases. As the current increases, the amount of material removed increases, resulting in more processing by-products, which accumulate in the machining gap due to the difficulty in by-products discharge, the resistance value in the processing area increases, and the processing capability weakens, and then the cylindrical taper angle increases. The cylindrical taper angles of the workpieces processed by the ECM with mask are larger than that of the workpieces processed by the ECM with tool sinking. In addition, as seen from the figure, under various machining current parameters, the cylindrical taper angles of the workpieces processed by the ECM with mask are larger than that of the workpieces processed by the ECM with tool sinking.

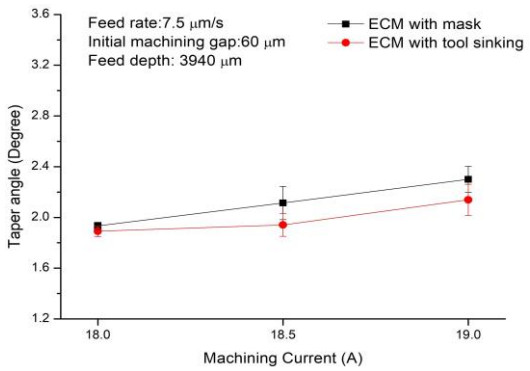

Fig. 10. The relationships between different processing methods and the cylindrical taper angle.

The Autodesk Computational Fluid Dynamics (CFD) simulation analysis software was used to analyze the flow field and flow velocity of the two processing methods. The simulation environment parameter settings are shown in Table V. Fig. 11 is the simulation diagram of the flow field direction and flow velocity at the bottom of the rectangular groove in the process of the two processing methods. As shown in Fig. 11, the flow velocity of the ECM with mask is lower than that of the ECM with tool sinking. The flow velocity around the cylinder in the ECM with mask is 200 cm/s, whereas the flow velocity around the cylinder can be increased to 350 cm/s by using the ECM with tool sinking. The lowest flow velocity is at the four corners of the rectangular groove. In the ECM with mask, the flow

velocity at the corners of the rectangular groove is 75 cm/s, whereas in the ECM with tool sinking, the flow velocity at the corners of the rectangular groove is increased to 135 cm/s. With a higher flow velocity in the machining gap, the electrolyte renewal efficiency is also higher, so that the processing heat and processing by-products can be more easily removed from the machining gap. In the ECM with tool sinking, the flow velocity in the processing area is higher than that in the ECM with mask, and the processing heat, bubbles, metal oxides and other processing products generated during the processing are easy to be removed from the processing area. Hence, the bottom of the processed rectangular groove has a better surface morphology, and the processed cylindrical taper angle is relatively small. The poor bottom morphology of the rectangular groove processed by the ECM with mask and large pits can be prevented. In addition, since only part of the surface of the workpiece after the ECM with mask is influenced by stray corrosion, there are color differences on the surface of the workpiece, which affect the appearance of the workpiece. Based on the above results, the workpiece processed by the ECM with tool sinking has better surface morphology and smaller cylindrical taper angle, so the ECM with tool sinking is used for the experiments on electrochemical trepanning of rectangular groove with inner cylindrical structure.

TABLE V. THE SIMULATION ENVIRONMENT PARAMETER SETTINGS

Parameters	Description
Inlet electrolyte flow rate (L/min)	0.5
Outlet electrolyte flow rate (L/min)	0.5
Electrolyte supply pressure (psi)	2.5
Machining gap when feeding to 3.94 mm (μm)	120

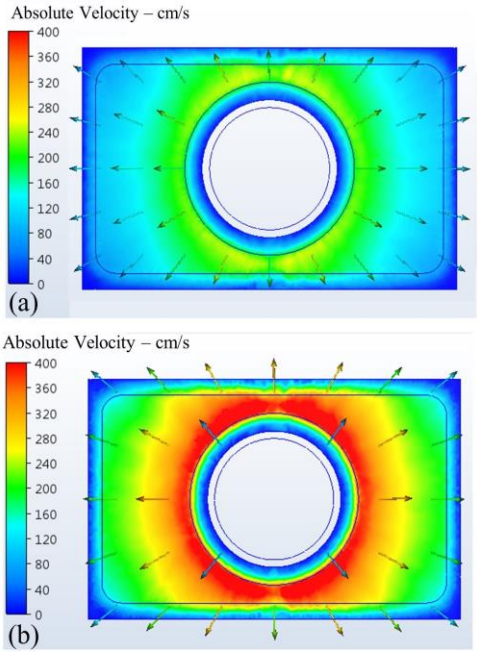

Fig. 11. The simulation diagram of the flow field direction and flow velocity at the bottom of the rectangular groove in the ECM process of the two processing methods. (a) ECM with mask. (b) ECM with tool sinking.

B. *Comparison of Electrochemical Trepanning with and without Ultrasonic Vibration Assistance*

As shown in Fig. 9, when the DC power supply is used for machining, the flow marks induced by the nonuniform flow field are likely to occur at the bottom of the rectangular groove, which degrade the surface quality of the bottom of the rectangular groove. The flow field nonuniformity can be improved by using pulse power supply and ultrasonic vibration assistance, so that the electrolyte renewal effect is better, and the ECM products can be removed better [21]. The machining using pulse power supply is supposed to eliminate the flow marks at the bottom of the rectangular groove. This section uses the pulse power supply to perform ECM with tool sinking of rectangular groove with inner cylindrical structure. Many studies discussed the benefits of ultrasonic vibration-assisted ECM to solve the problem of poor electrolyte renewal. Through different applications and technologies, the findings show that ultrasonic vibration assistance can significantly improve the quality of ECM. This section discusses the cylindrical taper angle, surface morphology and rectangular groove bottom surface roughness after the ECM with and without the ultrasonic vibration assistance. The parameter settings are shown in Table VI. The vibration amplitude of ultrasonic power Level 10 is 1.561 μm. Fig. 12 shows the surface morphology of the rectangular groove with inner cylinder with and without the ultrasonic vibration assistance. As seen from the figure, compared with the machining without the ultrasonic vibration assistance, at Amplitude 1.561 μm of ultrasonic power, the bottom of the rectangular groove is relatively bright. Fig. 13 shows the relationship of the cylindrical taper angle without ultrasonic vibration assistance and at amplitude 1.561 μm of ultrasonic power. Moreover, without ultrasonic vibration assistance, the cylindrical taper angle is 1.826°, and at amplitude 1.561 μm of ultrasonic power, the cylindrical taper angle is 1.717°. Compared with the case without ultrasonic vibration assistance, in the vibration assisted machining at Level 10 of ultrasonic power, the cylindrical taper angle decreases by 6%. When the ultrasonic vibration is applied to the sidewall-insulated electrode, the pumping effect and cavitation effect are generated, both of which disturb the electrolyte, promoting the electrolyte circulation, it is easier to remove the processing products, such as processing heat, bubbles and metal oxides. Compared with the machining without ultrasonic vibration assistance, as the ability to remove the processing products is better, at Level 10 of ultrasonic power, the cylindrical taper angle is smaller. In addition, as the heat and processing by-products in the processing area are easy to be removed, the resistance value in the machining gap is low, so that the current density increases accordingly. Therefore, at Level 10 of ultrasonic power, the bottom of the rectangular groove has a brighter surface. At Level 10 of ultrasonic power, the surface roughness of the bottom of the rectangular groove is 2.43 μmRa, while the surface roughness of the bottom of the rectangular groove without ultrasonic vibration assistance is Ra 3.35 μm. Compared ECM without ultrasonic vibration assistance, the surface

roughness of the ECM with the ultrasonic vibration assistance is better, as shown in Fig. 14. As seen, the roughness curve of the bottom of the rectangular groove in the machining with and without ultrasonic vibration assistance. In addition, in the ECM with tool sinking mode with the machining current of 18.5 A, the taper angle of the cylinder processed using DC current is 1.941°, while the taper angle of the cylinder processed using pulse power and ultrasonic vibration assistance is smaller than that processed using DC current. Compared with the experimental results in the previous section, the flow marks at the bottom of the rectangular groove are improved.

TABLE VI. THE PARAMETERS AND SETTING VALUES OF THE ECM WITH AND WITHOUT THE ULTRASONIC VIBRATION ASSISTANCE

Parameters	Description
Ultrasonic vibration amplitude (μm)	0, 1.561
Ultrasonic vibration frequency (kHz)	26.5
Machining current (A)	18.5
Current pulse frequency (Hz)	1000
Electrode feeding rate (μm/s)	4
Initial working gap (μm)	60
Electrode feeding stroke (μm)	3940
Duty factor (%)	50
Electrolyte concentration (wt.%)	10
Electrolyte temperature (°C)	30
Electrolyte supply pressure (psi)	2.5

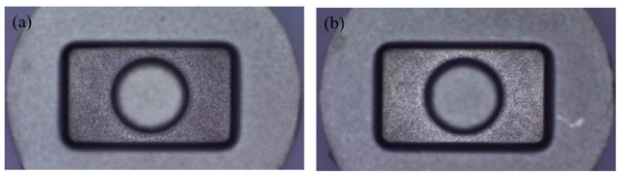

Fig. 12. The surface morphology of the rectangular groove with inner cylinder with and without the ultrasonic vibration assistance. (a) Without the ultrasonic vibration assistance. (b) With the ultrasonic vibration assistance.

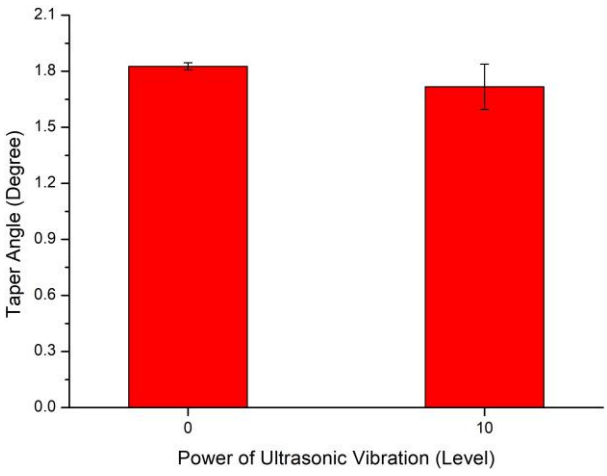

Fig. 13. The relationship of the cylindrical taper angle without ultrasonic vibration assistance and at amplitude 1.561 μm of ultrasonic power.

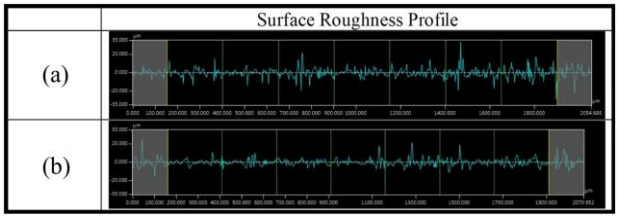

Fig. 14. The surface roughness of with and without the ultrasonic vibration assistance. (a) Without the ultrasonic vibration assistance. (b) With the ultrasonic vibration assistance.

To sum up the above results, the taper angle of the cylinder processed using pulse power supply and ultrasonic vibration-assisted processing is smaller than that without ultrasonic vibration-assisted processing, and the surface morphology and surface roughness of the processed rectangular groove with inner cylinder are better.

V. CONCLUSION

This study focused on ultrasonic-assisted electrochemical trepanning of rectangular groove with inner cylindrical structure. The experiments used the ECM with mask and ECM with tool sinking, and sidewall-insulated electrodes with and without ultrasonic vibration assistance to perform comparative experiments on the electrochemical trepanning of rectangular groove with inner cylindrical structure for SUS304 stainless steel, and discussed the influence of different processing methods on such quality characteristics as cylindrical taper angle and surface morphology. The results show that the combination of pulse current and ultrasonic vibration-assisted machining can improve the nonuniform flow field, accelerate the cyclic renewal of the electrolyte in the machining gap, and improve the machining accuracy of the rectangular groove with cylindrical structure. When the ultrasonic vibration is applied to the sidewall-insulated electrode, the pumping effect and cavitation effect are generated, both of which disturb the electrolyte, promoting the circulation of the electrolyte, it is easier to remove such processing by-products as processing heat, bubbles and metal oxides. Therefore, in comparison to the machining without ultrasonic vibration assistance, in the vibration assisted machining at amplitude 1.561 μm of ultrasonic power, the cylindrical taper angle decreases by 6%, and the rectangular groove with inner cylinder after processing has better surface morphology and surface roughness.

CONFLICT OF INTEREST

The authors declare no conflict of interest.

AUTHOR CONTRIBUTIONS

Conceptualization, Chun-Hao Yang and Hai-Ping Tsui; Methodology, Chun-Hao Yang; Data curation, Tzu-Yuan Chu; Visualization, Tzu-Yuan Chu; Investigation, Chun-Hao Yang and Hai-Ping Tsui; Supervision, A-Cheng Wang, Yan-Cherng Lin and Hai-Ping Tsui; Writing—review and editing, Chun-Hao Yang, A-Cheng Wang, Yan-Cherng Lin and Hai-Ping Tsui; Writing—original

draft preparation, Tzu-Yuan Chu; all authors had approved the final version.

FUNDING

The funding support of this work received from the National Science and Technology Council for funding the project. No. 112WFA0710552.

REFERENCES

[1] F. Klocke, M. Zeis, A. Klink, and D. Veselovac, "Experimental research on the electrochemical machining of modern titanium-and nickel-based alloys for aero engine components," *Procedia Cirp*, vol. 6, pp. 368–372, 2013.

[2] G. Zhouzhi, Z. Dong, X. Tingyu, L. Ao, and Z. Di, "Improvement of electrochemical trepanning by using a pictographic insulation sleeve," *International Journal of Electrochemical Science*, vol. 12, no. 11, pp. 10577–10588, 2017.

[3] X. Hu, D. Zhu, J. Li, and Z. Gu, "Flow field research on electrochemical machining with gas film insulation," *Journal of Materials Processing Technology*, vol. 267, pp. 247–256, 2019.

[4] C. Guo, J. Qian, and D. Reynaerts, "Electrochemical machining with Scanning Micro Electrochemical Flow Cell (SMEFC)," *Journal of Materials Processing Technology*, vol. 247, pp. 171–183, 2017.

[5] D. Wang, Z. Zhu, N. Wang, and D. Zhu, "Effects of shielding coatings on the anode shaping process during counter-rotating electrochemical machining," *Chinese Journal of Mechanical Engineering*, vol. 29, no. 5, pp. 971–976, 2016.

[6] J. Hung, H. Liu, Y. Chang, K. Hung, and S. Liu, "Development of helical electrode insulation layer for electrochemical microdrilling," *Procedia Cirp*, vol. 6, pp. 373–377, 2013.

[7] Z. Gu, D. Zhu, T. Xue, A. Liu, and D. Zhu, "Investigation on flow field in electrochemical trepanning of aero engine diffuser," *The International Journal of Advanced Manufacturing Technology*, vol. 89, pp. 877–884, 2017.

[8] W. Chen, F. Han, and J. Wang, "Influence of pulse waveform on machining accuracy in electrochemical machining," *The International Journal of Advanced Manufacturing Technology*, vol. 96, pp. 1367–1375, 2018.

[9] T. Koyano, A. Hosokawa, and T. Furumoto, "Analysis of electrochemical machining process with ultrashort pulses considering stray inductance of pulse power supply," *Journal of Advanced Mechanical Design, Systems, and Manufacturing*, vol. 12, no. 5, p. JAMDSM0098, 2018.

[10] Jing Wang, Zhengyang Xu, Jingtao Wang and Di Zhu, "Electrochemical machining on blisk channels with a variable feed rate mode," *Chinese Journal of Aeronautics*, vol. 34, no. 6, pp. 151–161, 2021.

[11] X. Jiang, J. Liu, D. Zhu, M. Wang, and N. Qu, "Research on stagger coupling mode of pulse duration and tool vibration in electrochemical machining," *Applied Sciences*, vol. 8, no. 8, pp. 1296, 2018.

[12] H. El-Hofy, "Vibration-assisted electrochemical machining: a review," *The International Journal of Advanced Manufacturing Technology*, vol. 105, no. 1–4, pp. 579–593, 2019.

[13] L. Ji, Y. Zhang, G. Wang, J. Zhang, and W. Yang, "Performance improvement of high-speed EDM and ECM combined process by using a helical tube electrode with matched internal and external flushing," *The International Journal of Advanced Manufacturing Technology*, vol. 117, pp. 1243–1262, 2021.

[14] A. Jerin and K. Karunakaran, "Machinability investigation and optimizing process parameters in ECM of stainless steel-12X18H10T for minimizing surface roughness," *Materials Today: Proceedings*, vol. 81, pp. 443–448, 2023.

[15] T. Shu, Y. Liu, K. Wang, T. Peng, and W. Guan, "Ultrasonic vibration-aided electrochemical drill-grinding of SLM-printed Hastelloy X based on analysis of its electrochemical behavior," *Electrochemistry Communications*, vol. 135, 107208, 2022.

[16] M. Wang, R. Zhang, Y. Shang, J. Zheng, X. Wang, and X. Xu, "Micro-milling microstructures in air-shielding ultrasonic assisted electrochemical machining," *Journal of Manufacturing Processes*, vol. 97, pp. 171–184, 2023.

[17] I. Yang, M. S. Park, and C. N. Chu, "Micro ECM with ultrasonic vibrations using a semi-cylindrical tool," *International Journal of Precision Engineering and Manufacturing*, vol. 10, pp. 5–10, 2009.

[18] W. Natsu, H. Nakayama, and Z. Yu, "Improvement of ECM characteristics by applying ultrasonic vibration," *International Journal of Precision Engineering and Manufacturing*, vol. 13, pp. 1131–1136, 2012.

[19] Z. Y. Shen and H. P. Tsui, "An investigation of ultrasonic-assisted electrochemical machining of micro-hole array," *Processes*, vol. 9, no. 9, 1615, 2021.

[20] S. Skoczypiec, "Research on ultrasonically assisted electrochemical machining process," *The International Journal of Advanced Manufacturing Technology*, vol. 52, pp. 565–574, 2011.

[21] J. B. Patel, Z. Feng, P. P. Villanueva, and W. N. Hung, "Quality enhancement with ultrasonic wave and pulsed current in electrochemical machining," *Procedia Manufacturing*, vol. 10, pp. 662–673, 2017.

[22] Z. Gu, W. Zhu, X. Zheng, and X. Bai, "Cathode tool design and experimental study on electrochemical trepanning of blades," *The International Journal of Advanced Manufacturing Technology*, vol. 100, pp. 857–863, 2019.

[23] Z. Dong, G. Zhouzhi, X. Tingyu, and L. Ao, "Simulation and experimental investigation on a dynamic lateral flow mode in trepanning electrochemical machining," *Chinese Journal of Aeronautics*, vol. 30, no. 4, pp. 1624–1630, 2017.